Generation of a Highly Active Folding Enzyme by Combining a Parvulin-Type Prolyl Isomerase from SurA with an Unrelated Chaperone Domain

Anne-Juliane Geitner, Edina Varga, Marc Wehmer and Franz X. Schmid

Laboratorium für Biochemie und Bayreuther Zentrum für Molekulare Biowissenschaften, *Universität Bayreuth, D-95440 Bayreuth, Germany*

Correspondence to Franz X. Schmid: *Biochemie, Universität Bayreuth, D-95440 Bayreuth, Germany.*
fx.schmid@uni-bayreuth.de
http://dx.doi.org/10.1016/j.jmb.2013.06.038
Edited by S. Radford

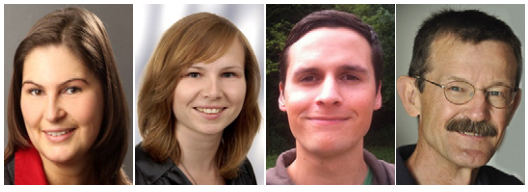

Anne-Juliane Geitner, Edina Varga, Marc Wehmer and Franz Xaver Schmid

Abstract

Parvulins are small prolyl isomerases and serve as catalytic domains of folding enzymes. SurA (survival protein A) from the periplasm of *Escherichia coli* consists of an inactive (Par1) and an active (Par2) parvulin domain as well as a chaperone domain. In the absence of the chaperone domain, the folding activity of Par2 is virtually abolished. We created a chimeric protein by inserting the chaperone domain of SlyD, an unrelated folding enzyme from the FKBP family, into a loop of the isolated Par2 domain of SurA. This increased its folding activity 450-fold to a value higher than the activity of SurA, in which Par2 is linked with its natural chaperone domain. In the presence of both the natural and the foreign chaperone domain, the folding activity of Par2 was 1500-fold increased. Related and unrelated chaperone domains thus are similarly efficient in enhancing the folding activity of the prolyl isomerase Par2. A sequence analysis of various chaperone domains suggests that clusters of exposed methionine residues in mobile chain regions might be important for a generic interaction with unfolded protein chains. This binding is highly dynamic to allow frequent transfer of folding protein chains between chaperone and catalytic domains.

Introduction

Slow steps in protein folding are catalyzed by enzymes such as thiol-disulfide oxido-reductases [1–4] or prolyl isomerases [5–8]. Usually, these enzymes consist of catalytic domains, which accelerate the respective slow folding steps, and of chaperone domains, which provide binding sites for the folding protein chains. Folding catalysts such as trigger factor [9], FKBP22 [10], or SlyD [11] consist of prolyl isomerase domains of the FKBP type and chaperone domains of varying size and structure. In most cases, the domains are contiguous along the protein chain, but in SlyD, the chaperone domain is inserted into a loop (the "flap") near the prolyl isomerase site of the FKBP domain. It is called the *insert-in-flap* or IF domain.

Human FKBP12 (12-kDa human FK506 binding protein) is naturally devoid of a chaperone domain. It is active as a prolyl isomerase with peptide substrates but almost inactive as a folding enzyme. Grafting the IF domain of SlyD into the flap loop of human FKBP12 increased its folding activity 200-fold [12]. Strong increases were also observed when foreign chaperone domains [from protein disulfide isomerase, GroEL, or SurA (survival protein A)] were inserted into human FKBP12. Apparently, this protein can be converted into a highly active folding catalyst by fusing it with a chaperone domain [13].

Parvulins constitute a different family of prolyl isomerases [14–16]. Here, we examined whether parvulin domains can also be transformed into folding enzymes by fusing them with chaperone domains. The SurA protein of *Escherichia coli* is a

periplasmic protein and participates in the maturation of outer membrane proteins [17–19]. It consists of two parvulin domains (Par1 and Par2) and a chaperone domain [20,21]. Par1 and Par2 are interleaved successively into the chaperone domain of this protein (Fig. 1a). Par1 is tightly associated with the chaperone domain and is apparently devoid of prolyl isomerase activity toward both peptide and protein substrates. Par2 resides in a protruding loop [20], and, in isolation, it shows prolyl isomerase activity when assayed with a tetrapeptide but is almost inactive as a catalyst of proline-limited protein folding [21].

Here, we analyzed how the folding activity of the Par2 domain of SurA changes when it is linked with a foreign chaperone domain (the IF domain of SlyD) instead of its own chaperone domain and how the activity of the Par2 domain responds to the presence of both the endogenous and the foreign chaperone domain. Remarkably, the foreign chaperone domain increased the activity of the Par2 domain in a protein folding assay more efficiently than its own chaperone domain.

Results

Design of chimeric proteins

For the construction of chimeras between the parvulin domains of SurA and a foreign chaperone domain, natural guidance could not be employed because parvulins with chaperone domains inserted close to the active site (as in the FKBP-type prolyl isomerase SlyD) are not known. To identify a loop near the catalytic center into which a chaperone domain could possibly be grafted, we exploited the structural homology between the parvulin domains of SurA and human Pin1 (Fig. 1b). Pin1 contains a prolyl isomerase domain of the parvulin type and is specific for phosphoserine or phosphothreonine

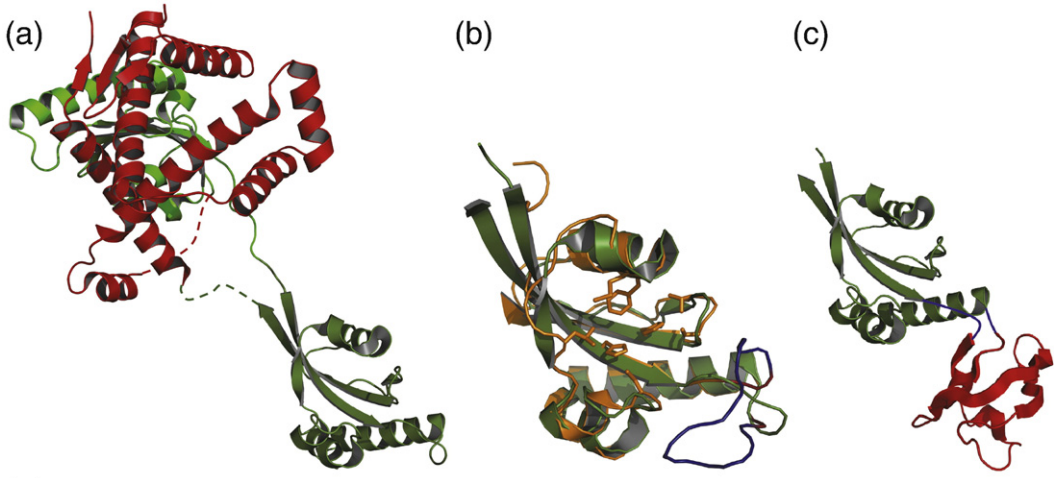

(d)

```
Pin1        51 -EPARVRCSHLLV-KHSQSRRPSSWRQEKITRTKE-----EALELINGYIQKIKSGEEDFESL
SurA Par1    2 ---TELNLSHILI-PLPENP----------TSDQVNEAESQARAIVDQA----RNGA-DFGKL
SurA Par2    2 ISVTEVHARHILL-KPS------------PIMTDE-----QARVKLEQIAADIKSGKTTFAAA
Par1+IF      2 ---TELNLSHILI-KHS--IF domain--TSDQVNEAESQARAIVDQA----RNGA-DFGKL
Par2+IF      2 ISVTEVHARHILL-KHS--IF domain--TRTDE-----QARVKLEQIAADIKSGKTTFAAA

Pin1       107 ASQFSDCSSAKAR-GDLGAFSRGQMQKPFEDASFALRTGEMSGPVFTDSGIHIILRTE------
SurA Par1  46 AIAHSADQ-QALNGGQMGWGRIQELPGIFAQALSTAKKGDIVGPIRSGVGFHILKVNDLRGES-
SurA Par2  47 AKEFSQDPGSANQGGDLGWATPDIFDPAFRDALTRLNKGQMSAPVHSSFGWHLIELLDTRNVDK
Par1+IF    105 AIAHSADQ-QALNGGQMGWGRIQELPGIFAQALSTAKKGDIVGPIRSGVGFHILKVNDLRGES-
Par2+IF    106 AKEFSQDPGSANQGGDLGWATPDIFDPAFRDALTRLNKGQMSAPVHSSFGWHLIELLDTRNVDK
```

Fig. 1. (a) The structure of SurA. The chaperone domain is shown in red, the Par1 domain (located behind the chaperone domain) is shown in light green, and the Par2 domain is shown in dark green. Unresolved linkers are indicated by broken lines. (b) Superimposition of the Par2 domain of SurA (dark green) and the parvulin domain of human Pin1 (orange). The extended loop of Pin1 that binds to phospho-Ser or phospho-Thr is shown in blue. The figure is enlarged relative to (a) and (c). (c) Schematic drawing of the chimeric protein Par2 + IF. Par2 is colored green, IF is in red, and the linkers taken from Pin1 are in blue. (d) Sequences of human Pin1 (hPin1), the Par1 and Par2 domains of SurA, and the chimeric proteins Par1 + IF and Par2 + IF. Loop residues of Pin1 are shown in blue. In the chimeric sequences, the inserted IF domain is colored red, and residues taken from Pin1 are shown in blue. Conserved residues used to align Par1 and Par2 with Pin1 are underlined. Residues implicated in catalysis are shown in stick representation in (b) and in boldface in (c). The Protein Data Bank files 1M5Y for SurA [20] and 1PIN for human Pin1 [15] and the program PyMOL [22] were used for (a) and (b).

Table 1. Stability data for the chimeric SurA variants

Protein	$[GdmCl]_{1/2}$ (M)	m (kJ mol^{-1} M^{-1})	ΔG_D 15 °C (kJ mol^{-1})
Par1	3.07 ± 0.15	9.3 ± 0.3	28.5 ± 0.7
Par1 + IF	1.15 ± 0.07	14.4 ± 0.5	16.5 ± 0.6
Par2	3.03 ± 0.17	13.4 ± 0.4	40.6 ± 1.1
Par2 + IF	1.89 ± 0.24	11.1 ± 0.7	21.0 ± 1.5

The transition midpoints $[GdmCl]_{1/2}$, the cooperativity parameters m, and the Gibbs free energies of denaturation at 15 °C $\Delta G_D^{15°C}$ were derived from the analysis of the GdmCl-induced unfolding transitions shown in Fig. S2. Unfolding was followed by fluorescence at 340 nm after excitation at 280 nm (Par1 and Par1 + IF) or by ellipticity at 222 nm (Par2 and Par2 + IF).

residues in front of the proline [15,23,24]. This specificity is mediated by a 12-residue extension of the loop between strand β1 and helix α1 (Fig. 1b). This loop is located near the catalytic site, and, apparently, it tolerates insertions. Based on the structure of human Pin1 [15] and the sequence alignment with the SurA Par1 and Par2 domains (Fig. 1d), we excised residues 16–20 (Par2 numbering) and replaced them by the chaperone (IF) domain of SlyD (residues 70–129). To optimize the linkers between Par2 and IF, we inserted residues from the sequence of Pin1 before and after the IF domain (Fig. 1d). In this manner, the IF domain of SlyD was inserted also into the isolated Par1 domain and into full-length SurA. A schematic representation of the chimeric protein Par2 + IF is shown in Fig. 1c.

Conformational stabilities of the chimeric proteins

At 15 °C, all chimeric variants showed CD spectra with minima between 205 and 220 nm and maxima near 190 nm, as typical for folded proteins (Fig. S1). The isolated domains Par1 and Par2 are highly stable. They show guanidinium chloride (GdmCl)-induced unfolding transitions with midpoints near 3 M, and they remain fully folded up to about 2 M GdmCl (Fig. S2). Proteins are generally destabilized by domain insertions, because the entropy of the unfolded state is increased [13,25–28]. Par1 and Par2 were destabilized by the insertion of the IF chaperone domain as well (Fig. S2), but both remained fully folded in the absence of denaturant (Table 1). The IF domain of SlyD is not stable in isolation [29,30]. Therefore, its unfolding is coupled with the unfolding of the Par domains, which explains the cooperative transitions of the chimeric proteins.

Prolyl isomerase activities in a peptide assay

To measure the prolyl isomerase activity of the SurA parvulin domains and of the chimeric proteins, we employed the assay with the tetrapeptide aminobenzoyl-Ala-Leu-Pro-Phe-4-nitroanilide (Abz-ALPF-*p*NA). In this assay, the time course of *cis*/*trans* isomerization is followed by the increase in Abz fluorescence [31,32], and the coupling with a protease as in the traditional prolyl isomerase assay [5] is avoided. In the fluorescence assay, the activity of the isolated Par1 domain was below the detection limit, as noted previously [21] with the protease-coupled assay.

The isolated Par2 domain was catalytically active but about ninefold less active than full-length SurA (Table 2). Previously, such a low activity had been measured for both SurA and the isolated Par2 domain with the protease-coupled assay. Apparently, the protease had cleaved full-length SurA rapidly during this assay, and thus the activity of the Par2 domain alone was measured in both cases [21]. The peptide activities of isolated Par2 and of the Par2 domain of intact SurA remained almost unchanged after insertion of the chaperone (IF) domain of SlyD (Table 2), although the site of insertion is near the prolyl isomerase active site and although the protein stability is decreased (Table 1).

Folding activities

The impact of the IF chaperone domain on the catalytic activity of the chimeric proteins as catalysts of proline-limited protein folding (the protein folding activity) was determined next. We used the reduced and carboxymethylated form of the S54G/P55N variant of ribonuclease T1 (RCM-T1) [33] as a substrate protein. It contains a single *cis* prolyl bond (Tyr38–Pro39) in its folded form [33–36]. In the absence of salt, RCM-T1 is unfolded, and refolding is started by increasing the NaCl concentration to 2.0 M. Fifteen percent of the unfolded RCM-T1

Table 2. Catalytic activities of the chimeric SurA variants

Protein	Peptide activity, k_{cat}/K_m (mM^{-1} s^{-1})	Folding activity, k_{cat}/K_m (mM^{-1} s^{-1})
Par1	n.d.	n.d.
Par1 + IF	n.d.	n.d.
Par2	53	0.15
Par2 + IF	74	69
SurA	460	38
SurA + IF	365	240

The k_{cat}/K_m values for peptide activity were determined by the increase in fluorescence of the peptide Abz-ALPF-*p*NA at 416 nm after excitation at 316 nm in 0.1 M potassium phosphate, pH 7.5, at 15 °C. The RCM-T1 refolding activity was followed by the increase in fluorescence at 320 nm after excitation at 268 nm in 0.1 M Tris–HCl and 2.0 M NaCl, pH 8.0, at 15 °C; n.d., not detectable. The precision of the k_{cat}/K_m values is ±10%.

molecules refold rapidly during the dead time of manual mixing, because they contain a correct *cis* Pro39. The remaining 85% refold slowly in a reaction that is limited in rate by the slow *trans*-to-*cis* isomerization at Pro39. It shows a time constant of 530 s (at 15 °C, pH 8.0) [33].

The isolated Par1 domain of SurA, which is inactive in the peptide assay, is inactive in the folding assay as well (Fig. 2a). Isolated Par2 shows a very low folding activity, and its catalytic efficiency (k_{cat}/K_m) as determined from the dependence of the measured folding rates on enzyme concentration (Fig. 2b) is only 0.15 mM^{-1} s^{-1} (Table 2), which is near the detection limit. It agrees with a value published earlier [21]. The insertion of the chaperone (IF) domain of SlyD into the Par2 domain increases its activity in the folding assay with RCM-T1 450-fold to 69 mM^{-1} s^{-1} (Fig. 2a). In the presence of its natural chaperone domain (in full-length SurA), the folding activity is 250-fold increased to 38 mM^{-1} s^{-1} (Table 2), which is also consistent with published data [21]. The foreign chaperone domain thus supported the protein folding activity of the SurA Par2 domain better than its natural chaperone domain as present in full-length SurA.

The variant SurA + IF contains both the natural and the foreign chaperone domain. It is an extremely powerful catalyst of folding when present at low nanomolar concentrations (Fig. 2c). SurA + IF (10 nM) accelerated the folding of RCM-T1 already 2-fold, and relative to the isolated Par2 domain, the protein folding activity increased 1500-fold (to 240 mM^{-1} s^{-1}). Above 100 nM SurA + IF, the rate of catalyzed folding no longer increased linearly but approached a limiting value. Presumably, progressive binding at the two chaperone domains interferes with productive refolding.

The linkage with one chaperone domain (as in Par2 + IF) or with two (as in SurA + IF) thus led to several-hundred-fold increases in the folding activity of the Par2 domain of SurA. This boost in folding activity required not only the binding to the chaperone domain but also a catalytically active prolyl isomerase domain. The inactive Par1 domain of SurA remained inactive in the protein folding assay even after coupling it in the same fashion with the same chaperone domains as the Par2 domain (Table 2).

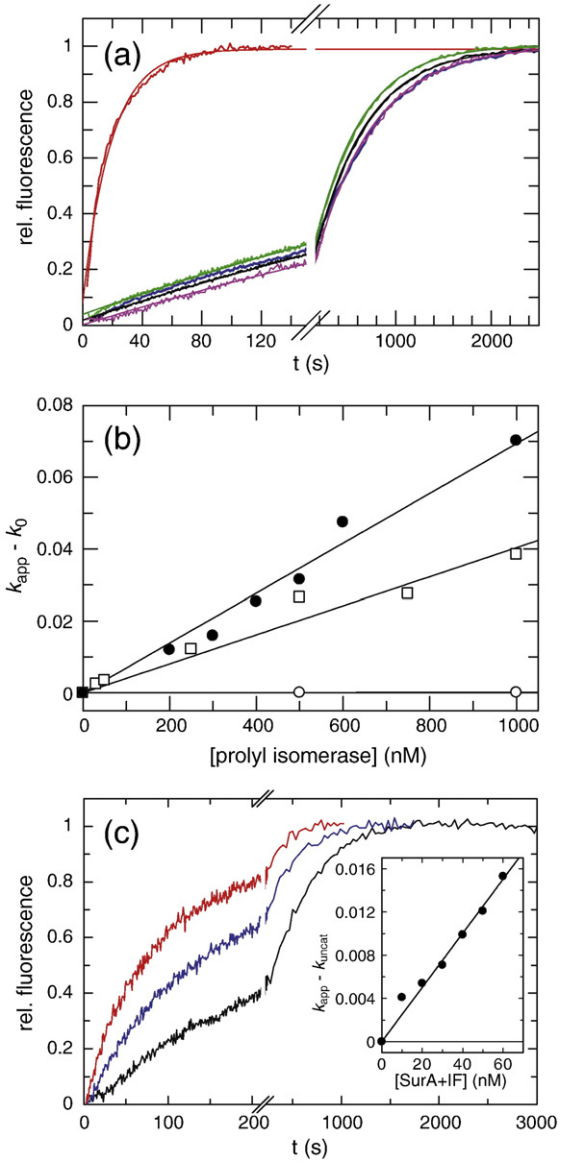

Fig. 2. Catalysis of the proline limited refolding of RCM-T1 by SurA variants. (a) Refolding in the absence of a prolyl isomerase (black) and in the presence of 1 μM of Par2 (green), Par2 + IF (red), Par1 (magenta), or Par1 + IF (blue). (b) Measured rate constants of catalyzed folding $k_{app} - k_0$ as a function of the concentration of Par2 (○), Par2 + IF (●), and SurA (□). (c) Kinetics of folding in the absence of a prolyl isomerase (black) and in the presence of 10 nM (blue) and 20 nM SurA + IF (red). The inset shows the measured rate constants of catalyzed folding $k_{app} - k_0$ as a function of the concentration of SurA + IF. The refolding of 0.1 μM RCM-T1 was followed by the increase in fluorescence at 320 nm after excitation at 268 nm in 0.1 M Tris–HCl and 2.0 M NaCl, pH 8.0 at 15 °C. The k_{cat}/K_m values derived from the slopes are given in Table 2.

Affinities of the SurA variants for unfolded proteins

The chaperone domains increase the catalytic efficiency (the k_{cat}/K_m value) of the Par2 domain in the protein folding assays presumably because they improve substrate binding. In simple Michaelis–Menten-type enzyme kinetics, K_m reflects the K_d value of the enzyme–substrate complex. To examine how the chimeric proteins with chaperone domains bind to an unfolded protein, we used an AEDANS [5-(((acetylamino)ethyl)amino)naphthalene-1-sulfonic acid]-labeled variant of ribonuclease

Table 3. Binding data for the interaction of AED-RNase T1 with the chimeric proteins

Variant	K_d[a] (μM)	k_{on}[b] (s^{-1} μM^{-1})	k_{off}[b] (s^{-1})	k_{off}/k_{on} (μM)	K_d[c] (μM)
SurA	1.2 ± 0.1	14.6 ± 0.7	124 ± 6	8.5 ± 0.8	2.2 ± 0.4
Par1 + IF	6.6 ± 0.5	16.2 ± 0.5	109 ± 5	6.8 ± 0.7	7.3 ± 0.5
Par2 + IF	10.1 ± 0.2				
SurA + IF	1.3 ± 0.1	19.3 ± 05	86 ± 5	4.4 ± 0.4	4.1 ± 0.5
SurA chaperone domain	0.8 ± 0.1	107 ± 4	140 ± 11	1.3 ± 0.2	2.6 ± 0.3
SlyD-D101W	1.2 ± 0.1	8.8 ± 0.5	10 ± 2	1.1 ± 0.2	2.6 ± 0.2

[a] These K_d values were calculated from equilibrium titrations as in Fig. S3 by assuming a 1:1 binding stoichiometry. Binding was monitored by the increase in AEDANS fluorescence at 475 nm after excitation at 280 nm (SurA and SurA + IF) or 295 nm (all others). Data for SlyD-D101W and the SurA chaperone domain were taken from Ref. [13].

[b] The microscopic rate constants of association k_{on} and dissociation k_{off} were derived from the dependence of the observed rate constant on the enzyme concentration as in Fig. 3d–f.

[c] These K_d values were calculated from the amplitudes of association kinetics as in Fig. 3g–i by assuming a 1:1 binding stoichiometry.

T1 (RNase T1) with seven substitutions (C2S, C6S, C10N, P39A, S54G, P55N, and W59F), termed AED-RNase T1. This form is permanently unfolded and devoid of Trp [13]. Thus, it is well suited to examine substrate binding, uncoupled from folding, by Förster resonance energy transfer. The domains Par1 and Par2 of SurA naturally contain one and two Trp residues, respectively, and an additional Trp

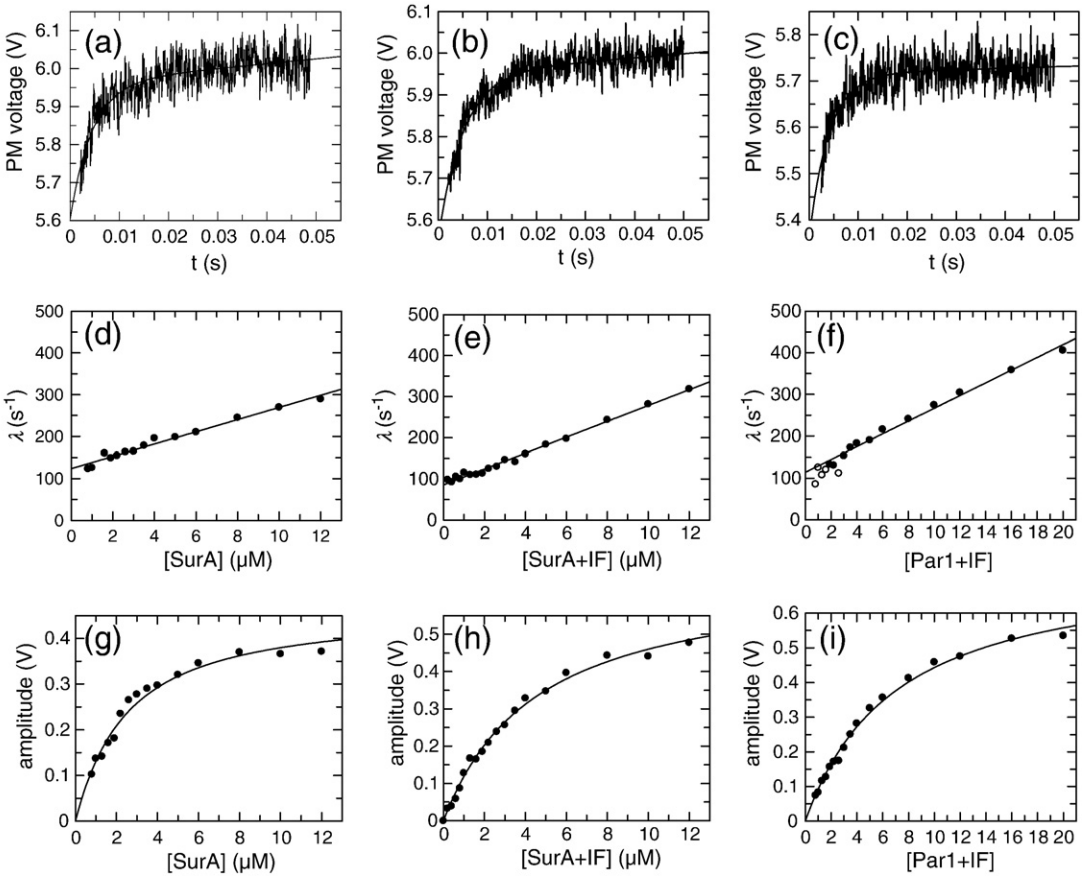

Fig. 3. Time course of complex formation between 0.5 μM AED-RNase T1 and 6 μM of (a) SurA, (b) SurA + IF, and (c) Par1 + IF. Data were analyzed by fitting monoexponential functions to the data. They gave k_{app} = 221 s^{-1} for SurA, 187 s^{-1} for SurA + IF, and 216 s^{-1} for Par1 + IF. The measured rate constants (d–f) and amplitudes (g–i) of complex formation are shown as a function of the concentration of SurA (d and g), SurA + IF (e and h), and Par1 + IF (f and i). Values for k_{off} and k_{on} were derived from the intercept and the slope of the lines in (d), (e), and (f), respectively. Values for K_d were derived from analyzing the amplitude data in (g), (h), and (i). The open symbols were not included into the data analysis. All data were analyzed assuming a 1:1 binding reaction. The kinetics were followed by fluorescence above 450 nm after excitation at 280 nm in 0.1 M Tris–HCl, pH 8.0, and 2.0 M NaCl at 15 °C. All equilibrium and rate constants derived from the analysis of the data are given in Table 3.

residue was inserted into the IF domains of Par1 + IF and Par2 + IF by the D101W substitution. Upon binding, energy is transferred from these Trp residues to the AEDANS group of AED-RNase T1, which was employed to study the equilibrium and the kinetics of the interactions between the different variants and AED-RNase T1.

Representative titration curves are shown in Fig. S3, the K_d values derived from the analyses are given in Table 3. The proteins that harbor the natural chaperone domain of SurA show the highest affinity for our permanently unfolded protein, with K_d values between 0.8 μM for the isolated SurA chaperone domain and 1.2 μM for SurA. In the additional presence of the IF domain (in SurA + IF), the K_d value (1.3 μM) is almost unchanged. Possibly, the measured titration curve (Fig. S3b) largely reflects the binding to the chaperone domain of SurA.

For the isolated prolyl isomerase domains Par1 and Par2 without a chaperone domain, evidence for binding could not be found. After the insertion of the IF domain of SlyD, the inactive variant Par1 + IF and the active variant Par2 + IF both bound to the permanently unfolded protein Fig. S3a. The K_d values were 6.6 and 10 μM, respectively (Table 3). In isolation, the IF domain is unfolded, and therefore its binding to the unfolded protein could not be measured. In SlyD, it shows a K_d of 1.2 μM for AED-RNase T1 (Table 3). The weaker affinity of the IF domain of Par1 + IF and Par2 + IF might be caused by a decreased accessibility of the binding site in these chimeric proteins. In summary, all SurA variants, with one or two chaperone domains, bound to the unfolded protein AED-RNase T1 with K_d values between 1 and 10 μM.

Kinetics of binding of the SurA variants to unfolded proteins

The interaction between SlyD and the unfolded protein AED-RNase T1 is characterized by high rates of association and dissociation [13], and we proposed that dynamic binding is important for an efficient substrate transfer between the chaperone domain and the catalytic domain and to avoid stalling by damaged proteins.

Figure 3a–c shows representative kinetics of binding of AED-RNase T1 to SurA, SurA + IF, and Par1 + IF, as well as the measured rate constants (Fig. 3d–f) and amplitudes (Fig. 3g–i) of association as a function of the protein concentration. The values for k_{on} are derived from the slope and those for k_{off} are derived from the intercepts in Fig. 3d–f. Table 3 shows the data from the kinetic analysis for all variants.

Full-length SurA binds to the unfolded protein very rapidly (Fig. 3a) with a k_{on} value $>10^7$ s^{-1} M^{-1} and a k_{off} >100 s^{-1} (Fig. 3d; Table 3), which implies that the average lifetime of the complex is less than 10 ms. For the isolated chaperone domain of SurA, the substrate binding dynamics is even higher [13]. It binds to AED-RNase T1 with an about sevenfold increased association rate constant ($k_{on} = 10^8$ s^{-1} M^{-1}, Table 3), which is close to the diffusion limit. The decreased k_{on} of full-length SurA thus originates probably from a lowered accessibility of its binding site. SurA + IF resembles SurA in the kinetics of substrate binding, presumably because the probe detects preferentially the interaction with the SurA chaperone domain (Table 3).

After the insertion of the IF chaperone domain into the isolated parvulin domains of SurA, the binding kinetics could be measured only for the inactive parvulin domain (Par1 + IF). For the active parvulin domain (Par2 + IF), the changes in fluorescence in the stopped-flow experiments were too small for a quantitative kinetic analysis. As a part of Par1 + IF, the IF domain reacted about twofold faster with the unfolded substrate protein than SlyD itself, which naturally harbors the IF domain (Table 3). The dissociation rate is approximately 10-fold increased, suggesting that the binding dynamics is increased even though the substrate affinity of the IF domain is decreased when it is inserted into the Par1 domain of SurA.

The kinetic data also provide information about the K_d values. K_d is equal to the ratio of the rate constants, k_{off}/k_{on}, and the amplitudes follow titration curves (Fig. 3g–i). Table 3 shows the K_d values from these analyses as well. In most cases, they are higher than the values derived from the equilibrium titrations, with the reason not being clear. Together, the kinetic data indicate that the high dynamics of substrate binding by the IF domain remained conserved after insertion into the Par1 or Par2 domains of SurA.

Discussion

Domains for the binding of unfolded protein substrates, loosely termed chaperone domains, are important for prolyl isomerases to function as protein folding enzymes, and the excision of the chaperone domains from SlyD or from SurA almost abolished their folding activities. The reciprocal insertion of the SlyD chaperone (IF) domain into the human homolog FKBP12 increased its folding activity 200-fold [12], indicating that the IF domain of SlyD can cooperate with a related FKBP domain. Other chaperone domains such as those from protein disulfide isomerase, GroEL, or SurA also improved the folding activity of FKBP12 but were less efficient than the IF domain of SlyD [13].

SurA is a parvulin-type prolyl isomerase. Its Par1 domain is inactive in isolation and remains inactive when linked with its natural chaperone domain in intact SurA or with the IF domain of SlyD, even

though intact SurA and the chimera Par1 + IF bind to unfolded proteins with high affinity.

The folding activity of the Par2 domain of SurA is 250-fold increased by its own chaperone domain and 450-fold by the IF domain of SlyD when inserted artificially into a loop near the prolyl isomerase active site. It is remarkable that the foreign chaperone domain is more efficient than the endogenous chaperone domain. In the crystal structure of SurA [20], the Par2 domain extends away from its chaperone domain (Fig. 1a). The distance between the protein binding and the prolyl isomerase sites might thus be larger in SurA than in the artificial chimera Par2 + IF, and accordingly, substrate transfer might be less efficient. However, in the absence of structural information for the chimeric construct, this remains a speculation. Additional aspects such as the relative orientation and mobility of the domains in solution might be important as well.

When both chaperone domains are present, as in SurA + IF, the folding activity of the Par2 domain is further enhanced. This indicates that the two chaperone domains do not compete with each other for substrate binding. Rather, they cooperate and lead to a 1500-fold increase in folding activity. By providing two protein binding sites, they increase the probability of capturing substrate for the transfer to the active site. They also increase the probability that protein molecules that leave the prolyl isomerase active site with an incorrect prolyl isomer are bound again and thus rerouted back for an additional round of catalysis. At both chaperone domains, the refolding protein molecules bind and dissociate very rapidly. Thus, adverse effects on productive folding caused by overly strong binding are avoided.

The chaperone (IF) domain of SlyD activates its own FKBP domain, human FKBP12 [12], and the unrelated parvulin-type prolyl isomerase domain Par2 of SurA in a similar fashion. In all cases, the IF domain bound to refolding protein molecules in a highly dynamic fashion and increased the folding activity more than 100-fold.

The IF domains of SlyD or the SlyD-like protein SlpA probably use a groove formed by helix 3 and the β8–β9 loop (Fig. 4) for substrate binding [11,38–40]. These two elements of structure (colored red in Fig. 4) show the highest backbone mobility within the IF domain, as indicated by heteronuclear $^{1}H–^{15}N$ NOE effects lower than 0.6 in solution [11,37]. Unlike the other parts of SlyD, helix 3 and the β8–β9 loop of IF are rich in exposed methionine residues. SlyD variants from various bacteria [41] constantly show between two and four methionine residues in this presumed substrate binding region. Interestingly, these residues (marked in green, Fig. 4) are not at conserved positions in the SlyD homologs but occupy variable locations along the substrate binding groove.

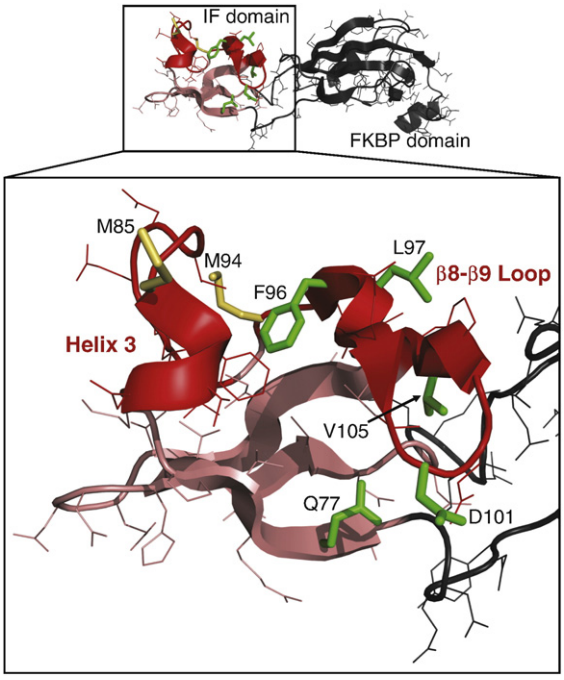

Fig. 4. Structure of the IF domain of SlyD. The mobile regions (helix 3 and the β8–β9 loop) with heteronuclear $^{1}H–^{15}N$ NOE effects lower than 0.6 [11,37] are shown in red. M85 and M94 of SlyD from *E. coli* are shown in yellow, and the side chain of residues that are changed to Met in SlyD homologs are shown in green. The figure was prepared by using the Protein Data Bank file 2K8I [11].

Unusually high numbers of Met residues occur also in the chaperone domains of SurA (11 Met) [20] and of trigger factor (5 Met) [9]. Flexible methionine residues in mobile regions of a protein are ideally suited for creating adaptive sites for the generic binding to stretches of hydrophobic residues. In fact, arrays of Met residues (“methionine bristles”) in flexible chain segments are used by the signal recognition particle to interact with a wide array of hydrophobic sequences [42–44]. Presumably, the IF domains of the SlyD homologs and the chaperone domains of other folding enzymes use the same principle for the adaptive binding to hydrophobic patches that are exposed in unfolded or incompletely folded protein substrates.

The backbone of the IF domain remains mobile even after substrate binding [37], which agrees well with our finding that binding is very fast and not followed by a lock-in step. The bound protein substrate thus stays mobile as well, and the rates of association and dissociation remain high. This is an essential prerequisite for the rapid transfer of the bound protein molecules to the catalytic site and is important for the proper function of folding enzymes.

Materials and Methods

Materials

GdmCl (ultrapure) was obtained from ICN Biomedicals (Aurora, OH, USA). Isopropyl β-D-1-thiogalactopyranoside was purchased from Gerbu (Haiberg, Germany); IAEDANS was from Invitrogen (Darmstadt, Germany). All other chemicals were from Roth (Karlsruhe, Germany) or Grüssing (Filsum, Germany). The Abz-ALPF-*p*Na peptide was a gift from Dr. Tobias Aumüller (Technische Universität München). Fluorescence and CD were measured by using a Jasco FP-6500 fluorescence spectrometer and a Jasco J-600A spectropolarimeter, respectively.

Expression and purification of proteins

The gene fragments encoding the isolated parvulin domains (Par1, Par2) were amplified from the corresponding genes and cloned into the expression plasmid pET11a. The gene fragment of SurA was cloned into the expression plasmid pET24a. For the chimeric proteins, the gene fragment of the IF domain (residues 70–128 of SlyD) was inserted into the gene of SurA and the parvulin domains via overlap extension PCR. Recombinant Par1, Par2, Par1 + IF, and Par2 + IF were linked N-terminally with the SUMO protein Smt3 from *Saccharomyces cerevisiae* containing an N-terminal hexahistidine tag to facilitate Ni-NTA-based purification [45]. The fusion proteins were overproduced in *E. coli* BL21(DE3) (Stratagene, Santa Clara, CA, USA). After lysis of the cells in 50 mM Tris–HCl, 50 mM NaCl, and 10 mM ethylenediaminetetraacetic acid, pH 8.0, with a microfluidizer and centrifugation, the SUMO fusion proteins were obtained in a soluble form. The fusion proteins were purified by immobilized metal-affinity chromatography on a Ni-NTA column (elution with 250 mM imidazole) and cleaved with 1 μM of a fragment of the SUMO protease Ulp1 overnight at 4 °C. The SUMO fragment was removed by a second passage over a Ni-NTA column, and the protein variants were further purified by gel filtration on a Superdex 75 prep-grade column (GE Healthcare, Uppsala, Sweden). SurA and SurA + IF were purified in a similar way, yielding the pure proteins after immobilized metal-affinity chromatography on a Ni-NTA column followed by gel filtration on a Superdex 75 prep-grade column (GE Healthcare). (S54G,P55N)-RNase-T1 was expressed, purified, reduced, and carboxymethylated under denaturing conditions, as described previously [33]. (C2S,C6S,C10N, P39A,S54G,P55N,W59F)-RNaseT1 was expressed, purified, and modified with IAEDANS (AED-RNase T1) as described previously [13].

Equilibrium unfolding transitions

Samples of the protein variants (1 or 2 μM) were incubated for 1 h at 15 °C in 0.1 M potassium phosphate, pH 7.5, and varying concentrations of GdmCl. The transitions of Par1 and Par1 + IF were measured by fluorescence in 10-mm cells at 340 nm with 5-nm bandwidth, after excitation at 280 nm (3 nm bandwidth). The transitions of Par2 and Par2 + IF were measured by CD at 222 nm in 10-mm cells with a bandwidth of 1 nm. The unfolding transitions were analyzed on the basis of a two-state model and assuming a linear dependence of the Gibbs free energy on denaturant concentration [46].

Peptide assay for prolyl isomerase activity

The prolyl isomerase activities of the proteins were measured by a protease-free assay as previously described [32]. For the assay, 750 μM of the peptide substrate Abz-ALPF-*p*Na was dissolved in anhydrous trifluoroethanol containing 0.55 M LiCl. Under these conditions, approximately 50% of the peptide molecules are in the *cis* conformation. Upon dilution with aqueous buffer (0.1 M potassium phosphate, pH 7.5), the *cis* content decreases to 10%. The corresponding shift of the *cis*/*trans* equilibrium was followed at a peptide concentration of 3 μM by the increase in fluorescence at 416 nm (5 nm bandwidth) after excitation at 316 nm (3 nm bandwidth) in 10-mm cells at 15 °C. The K_m value for the assay peptide could not be determined, due to the limited solubility, but it is larger than 50 μM. The peptide concentration in the assays was much smaller and catalyzed *cis*/*trans* isomerization of the prolyl bond was therefore a monoexponential process, and its rate constant increased linearly when plotted as a function of the prolyl isomerase concentration. The catalytic efficiency k_{cat}/K_m was determined from the slope of this plot. In these experiments, the enzyme concentrations were typically varied between 0 and 1 μM.

Catalysis of proline-limited protein refolding

For the protein refolding assays, RCM-T1 was unfolded by incubating 10 μM protein in 0.1 M Tris–HCl, pH 8.0, at 15 °C for at least 1 h. Refolding at 15 °C was initiated by a 100-fold dilution to final conditions of 0.1 μM RCM-T1 in 2.0 M NaCl, 0.1 M Tris–HCl, pH 8.0, and the desired concentrations of the prolyl isomerase. The slow folding reaction was followed by measuring the increase in protein fluorescence at 320 nm (5 nm bandwidth) after excitation at 268 nm (3 nm bandwidth). In the refolding assay, the small contribution of the prolyl isomerases to the fluorescence was subtracted from the measured values. The concentration of the substrate RCM-T1 (0.1 μM) was lower than the K_m value and therefore the measured rate of folding k_{app} increased linearly as a function of the prolyl isomerase concentration. The measured rate of folding, k_{app}, is equal to the sum of the rate of the uncatalyzed (k_0) and the rate of the catalyzed reaction. The latter rate is equal to $(k_{cat}/K_m)\cdot[E]_0$ [Eq. (1)] when the substrate concentration is much lower than the K_m value, as in this case.

$$k_{app} = k_0 + \frac{k_{cat}}{K_m}\cdot[E]_0 \qquad (1)$$

The catalytic efficiency k_{cat}/K_m could thus be determined from the slope when $k_{app} - k_0$ was plotted as a function of the enzyme concentration $[E]_0$. In these experiments, the prolyl isomerase concentrations were typically varied between 0 and 1 μM.

Equilibrium and kinetic measurements of substrate association

The titrations of 1 μM AED-RNase T1 with SurA or the chimeric variants were followed by the increase in the

fluorescence of AED-RNase T1 at 475 nm (5 nm bandwidth) upon energy transfer from the Trp residues of SurA and the variants.

Excitation was at 280 nm (SurA and SurA + IF) or 295 nm (all others) with a bandwidth of 3 nm. The kinetics of binding were measured after stopped-flow mixing using a DX.17MV stopped-flow spectrometer from Applied Photophysics (Leatherhead, UK). The path length of the observation chamber was 2 mm, and a 10-mM solution of *p*-nitroaniline in ethanol in a 5-mm cell was inserted in front of the emission photomultiplier to absorb scattered light from the excitation beam and fluorescence below 450 nm. The kinetics were followed by fluorescence above 450 nm after excitation at 280 nm (10 nm bandwidth). Kinetic curves were measured 10 times under identical conditions, averaged, and analyzed as monoexponential functions.

Minor drifts of the final values in the stopped-flow experiments were accounted for by adding a linear term to the equation used for the analysis. All binding experiments were performed in 0.1 M Tris–HCl and 2.0 M NaCl, pH 8.0, at 15 °C. The titration curves and the profiles obtained for the binding amplitudes were analyzed by assuming a 1:1 binding stoichiometry with the quadratic Eq. (1)

$$F - F_0 = (F_\infty - F_0) \cdot \frac{[P]_0 + [S]_0 + K_d - \sqrt{([P]_0 + [S]_0 + K_d)^2 - 4 \times [P]_0 \times [S]_0}}{2[P]_0}$$

in which F is the measured fluorescence and F_0 and F_∞ are the initial and final values, respectively. $[P]_0$ and $[S]_0$ are the protein and substrate concentrations, respectively. The program GraFit 5.0 (Erithacus Software, Staines, UK) was used for the analysis.

Acknowledgements

We thank Tobias Aumüller for the Abz-ALPF-*p*NA peptide, Jochen Balbach, Johanna Koch, Philipp Schmidpeter, Christian Scholz, and Gabriel Zoldák for suggestions and comments on the manuscript. This research was supported by grants from the Deutsche Forschungsgemeinschaft.

Supplementary Data

Supplementary data to this article can be found online at http://dx.doi.org/10.1016/j.jmb.2013.06.038

Received 3 May 2013;
Received in revised form 17 June 2013;
Accepted 20 June 2013
Available online 17 July 2013

Keywords:
protein folding;
folding catalysis;
SlyD;
artificial enzyme;
domain insertion

Abbreviations used:
FKBP12, 12-kDa human FK506 binding protein; IF, insert-in-flap; SurA, survival protein A; RNase T1, ribonuclease T1; RCM-T1, the reduced and carboxymethylated form of the S54G/P55N variant of ribonuclease T1; Abz, aminobenzoyl; *p*NA, *para*-nitroanilide; AEDANS, 5-(((acetylamino)ethyl)amino)naphthalene-1-sulfonic acid; GdmCl, guanidinium chloride.

References

[1] Venetianer P, Straub FB. The enzymic reactivation of reduced ribonuclease. Biochim Biophys Acta 1963;67:166–8.
[2] Goldberger RF, Epstein CJ, Anfinsen CB. Acceleration of reactivation of reduced bovine pancreatic ribonuclease by a microsomal system from rate liver. J Biol Chem 1963;238:628–35.
[3] Tian G, Xiang S, Noiva R, Lennarz WJ, Schindelin H. The crystal structure of yeast protein disulfide isomerase suggests cooperativity between its active sites. Cell 2006;124:61–73.
[4] Gruber CW, Cemazar M, Heras B, Martin JL, Craik DJ. Protein disulfide isomerase: the structure of oxidative folding. Trends Biochem Sci 2006;31:455–64.
[5] Fischer G, Bang H, Mech C. Nachweis einer Enzymkatalyse für die *cis–trans*-Isomerisierung der Peptidbindung in prolinhaltigen Peptiden. Biomed Biochim Acta 1984;43:1101–11.
[6] Lang K, Schmid FX, Fischer G. Catalysis of protein folding by prolyl isomerase. Nature 1987;329:268–70.
[7] Schmid FX. Prolyl isomerases. Adv Protein Chem 2002;59:243–82.
[8] Schmid FX. Prolyl isomerization in protein folding. In: Buchner JKT, editor. Protein folding handbook. Weinheim: Wiley-VCH; 2005. p. 916–45.
[9] Ferbitz L, Maier T, Patzelt H, Bukau B, Deuerling E, Ban N. Trigger factor in complex with the ribosome forms a molecular cradle for nascent proteins. Nature 2004;431:590–6.
[10] Saul FA, Arie JP, Vulliez-le Normand B, Kahn R, Betton JM, Bentley GA. Structural and functional studies of FkpA from *Escherichia coli*, a *cis*/*trans* peptidyl-prolyl isomerase with chaperone activity. J Mol Biol 2004;335:595–608.
[11] Weininger U, Haupt C, Schweimer K, Graubner W, Kovermann M, Brüser T, et al. NMR solution structure of SlyD from *Escherichia coli*: spatial separation of prolyl isomerase and chaperone function. J Mol Biol 2009;387:295–305.
[12] Knappe TA, Eckert B, Schaarschmidt P, Scholz C, Schmid FX. Insertion of a chaperone domain converts FKBP12 into a powerful catalyst of protein folding. J Mol Biol 2007;368:1458–68.
[13] Geitner AJ, Schmid FX. Combination of the human prolyl isomerase FKBP12 with unrelated chaperone domains leads to chimeric folding enzymes with high activity. J Mol Biol 2012;420:335–49.

[14] Rahfeld J-U, Schierhorn A, Mann K-H, Fischer G. A novel peptidyl–prolyl *cis*/*trans* isomerase from *Escherichia coli*. FEBS Lett 1994;343:65–9.
[15] Ranganathan R, Lu KP, Hunter T, Noel JP. Structural and functional analysis of the mitotic rotamase Pin1 suggests substrate recognition is phosphorylation dependent. Cell 1997;89:875–86.
[16] Sekerina E, Rahfeld JU, Müller J, Fanghänel J, Rascher C, Fischer G, et al. NMR solution structure of hPar14 reveals similarity to the peptidyl prolyl *cis*/*trans* isomerase domain of the mitotic regulator hPin1 but indicates a different functionality of the protein [In Process Citation]. J Mol Biol 2000;301:1021–35.
[17] Rouviere PE, Gross CA. SurA, a periplasmic protein with peptidyl-prolyl isomerase activity, participates in the assembly of outer membrane porins. Gene Dev 1996;10:3170–82.
[18] Missiakas D, Betton JM, Raina S. New components of protein folding in extracytoplasmic compartments of *Escherichia coli* SurA, FkpA and Skp/OmpH. Mol Microbiol 1996;21:871–84.
[19] Lazar SW, Kolter R. SurA assists the folding of *Escherichia coli* outer membrane proteins. J Bacteriol 1996;178:1770–3.
[20] Bitto E, McKay DB. Crystallographic structure of SurA, a molecular chaperone that facilitates folding of outer membrane porins. Structure 2002;10:1489–98.
[21] Behrens S, Maier R, de Cock H, Schmid FX, Gross CA. The SurA periplasmic PPIase lacking its parvulin domains functions *in vivo* and has chaperone activity. EMBO J 2001;20:285–94.
[22] DeLano WL. The PyMOL molecular graphics system. DeLano Scientific LLC. San Carlos, CA, USA: DeLano Scientific; 2003.
[23] Lu KP, Hanes SD, Hunter T. A human peptidyl–prolyl isomerase essential for regulation of mitosis. Nature 1996;380:544–7.
[24] Yaffe MB, Schutkowski M, Shen MH, Zhou XZ, Stukenberg PT, Rahfeld JU, et al. Sequence-specific and phosphorylation-dependent proline isomerization—a potential mitotic regulatory mechanism. Science 1997;278:1957–60.
[25] Ay J, Gotz F, Borriss R, Heinemann U. Structure and function of the *Bacillus* hybrid enzyme GluXyn-1: native-like jellyroll fold preserved after insertion of autonomous globular domain. Proc Natl Acad Sci USA 1998;95:6613–8.
[26] Aroul-Selvam R, Hubbard T, Sasidharan R. Domain insertions in protein structures. J Mol Biol 2004;338:633–41.
[27] Radley TL, Markowska AI, Bettinger BT, Ha JH, Loh SN. Allosteric switching by mutually exclusive folding of protein domains. J Mol Biol 2003;332:529–36.
[28] Ha JH, Butler JS, Mitrea DM, Loh SN. Modular enzyme design: regulation by mutually exclusive protein folding. J Mol Biol 2006;357:1058–62.
[29] Zoldák G, Carstensen L, Scholz C, Schmid FX. Consequences of domain insertion on the stability and folding mechanism of a protein. J Mol Biol 2009;386:1138–52.
[30] Haupt C, Weininger U, Kovermann M, Balbach J. Local and coupled thermodynamic stability of the two-domain and bifunctional enzyme SlyD from *Escherichia coli*. Biochemistry 2011;50:7321–9.
[31] Garcia-Echeverria C, Kofron JL, Kuzmic P, Kishore V, Rich DH. Continuous fluorimetric direct (uncoupled) assay for peptidyl prolyl *cis*-*trans*-isomerases. J Am Chem Soc 1992;114:2758–9.
[32] Zoldák G, Aumüller T, Lücke C, Hritz J, Oostenbrink C, Fischer G, et al. A library of fluorescent peptides for exploring the substrate specificities of prolyl isomerases. Biochemistry 2009;48:10423–36.
[33] Mücke M, Schmid FX. Folding mechanism of ribonuclease T1 in the absence of the disulfide bonds. Biochemistry 1994;33:14608–19.
[34] Kiefhaber T, Grunert HP, Hahn U, Schmid FX. Replacement of a cis proline simplifies the mechanism of ribonuclease T1 folding. Biochemistry 1990;29:6475–80.
[35] Mayr LM, Odefey C, Schutkowski M, Schmid FX. Kinetic analysis of the unfolding and refolding of ribonuclease T1 by a stopped-flow double-mixing technique. Biochemistry 1996;35:5550–61.
[36] Mücke M, Schmid FX. Enzymatic catalysis of prolyl isomerization in an unfolding protein. Biochemistry 1992;31:7848–54.
[37] Kovermann M, Zierold R, Haupt C, Löw C, Balbach J. NMR relaxation unravels interdomain crosstalk of the two domain prolyl isomerase and chaperone SlyD. Biochim Biophys Acta 2011;1814:873–81.
[38] Löw C, Neumann P, Tidow H, Weininger U, Haupt C, Friedrich-Epler B, et al. Crystal structure determination and functional characterization of the metallochaperone SlyD from *Thermus thermophilus*. J Mol Biol 2010;398:375–90.
[39] Haupt C, Patzschke R, Weininger U, Gröger S, Kovermann M, Balbach J. Transient enzyme–substrate recognition monitored by real-time NMR. J Am Chem Soc 2011;133:11154–62.
[40] Quistgaard EM, Nordlund P, Löw C. High-resolution insights into binding of unfolded polypeptides by the PPIase chaperone SlpA. FASEB J 2012;26:4003–13.
[41] Scholz C, Eckert B, Hagn F, Schaarschmidt P, Balbach J, Schmid FX. SlyD proteins from different species exhibit high prolyl isomerase and chaperone activities. Biochemistry 2006;45:20–33.
[42] Bernstein HD, Poritz MA, Strub K, Hoben PJ, Brenner S, Walter P. Model for signal sequence recognition from amino-acid sequence of 54K subunit of signal recognition particle. Nature 1989;340:482–6.
[43] Keenan RJ, Freymann DM, Walter P, Stroud RM. Crystal structure of the signal sequence binding subunit of the signal recognition particle. Cell 1998;94:181–91.
[44] Batey RT, Rambo RP, Lucast L, Rha B, Doudna JA. Crystal structure of the ribonucleoprotein core of the signal recognition particle. Science 2000;287:1232–9.
[45] Mossessova E, Lima CD. Ulp1-SUMO crystal structure and genetic analysis reveal conserved interactions and a regulatory element essential for cell growth in yeast. Mol Cell 2000;5:865–76.
[46] Santoro MM, Bolen DW. Unfolding free energy changes determined by the linear extrapolation method. 1. Unfolding of phenylmethanesulfonyl a-chymotrypsin using different denaturants. Biochemistry 1988;27:8063–8.